2010 IEEE International Conference on Robotics and Automation
Anchorage Convention District
May 3-8, 2010, Anchorage, Alaska, USA

Kinematic path-following control of a mobile robot on arbitrary surface

Gavin Kane, Robert Boesecke, Jörg Raczkowsky and Heinz Wörn

Abstract— **This paper outlines a method for applying a kinematic path following control of a mobile robot without any regard for surface structure. Background. A great deal of mobile robotics kinematics analysis is based on the movement of the robot on a two dimensional flat surface. Our application for precision surgery required a new approach to a system that would operate on a highly non-linear surface; this specific system was a surgical robot that would conduct craniotomies while moving over highly irregular and often deformed skulls. Methods. The approach used an abstract view of the operating environment that would totally ignore the surface, instead determining the control parameters based only on the robot and the desired cutting trajectory. The approach was then evaluated in a 3D environment using a series of predefined surfaces to determine bounding limits in the control theory. These limits were then tested in a second series of tests using real data from the CT preoperative imagery of previous patients and phantoms. The simulation results were then compared with the actual performance of the robot on phantoms and cadavers. Results. The approach has been successfully implemented on the first medical robot to position itself through spiked wheels on the surface of the skull. Testing has to date been successful in both a simulation environment, and on initial phantom and cadiever trials, with accuracies equal to that of the larger industrial modified surgical robots.**

I. BACKGROUND

1) Mobile Robots in Medicine: Mobile Robots have been employed in a number of roles within the health industry. Examples include service robots for delivery of specimens from the patient to the laboratory or medicaments to the patient. Presently the use of mobile robotics in precision critical applications in surgery is non-existent. This area of robotics has been the domain of large modified industrial robots where their high degree of precision is of the greatest benefit. Many other smaller and novel systems have arisen through the years, and have been given the title of Steady Hand Surgical Assistants. Examples as early as 1999 by Taylor et al. [1] presented the concept for reducing hand tremors and for overcoming human sensorimotor limitations. However, the side-effect for using the smaller systems, was a smaller work space available on the patient.

2) The Craniotomy and previous research efforts: There are a number of reasons for attempting to perform a highly accurate surgical craniotomy in accordance with a plan. Three examples include minimally invasive neurosurgery procedures (where the desired entry hole is pre-planned), frontal orbital advancement procedures for cranio- and maxillo-facial surgery (where the desired cranium advancement is pre-planned), or more recently post-traumatic or plastic surgery cranial reconstructions [2] (where the insertion area for a prefabricated implant [3] needs to be prepared very accurately according to a 3D CAD/CAM plan.)

Previous research efforts have concentrated on the use of modified industrial robots; however, they generally posed three main disadvantages:

1) Modified industrial robots generally exhibit a high impact within the OR. This is in terms of realestate required and the changes to surgical workflows that need to be adopted.
2) Robots milling craniotomies with unconstrained 6 DOF milling have considerable risk. Even with virtual fixtures defined in software, it requires only a minor registration error to cut too deep. This risk of causing meninges tears, and possibly thereafter damage to the brain is rarely accepted in practice.
3) Current examples of surgical robot systems [[3], [4], [5]] demonstrate a predominance of supervisory controlled interventions with the robot per-

This work was supported by the Marie Curie EU Funding under FP6.

Gavin Kane, Prof. Raczkowsky and Prof. Wörn are with the Institute of Process Control and Robotics, University of Karlsruhe, 76227 Karlsruhe, Germany

Dr. R. Boesecke is with the Department of Cranio Maxillo Facial Surgery, University Hospital of Heidelberg, 69120 Heidelberg, Germany

Corresponding Author - Gavin Kane MEngSc, University of Karlsruhe gavin@ira.uka.de

forming the pre-planned and programmed movements autonomously. This removes the surgeon from the procedure at the key time when his/her years of experience are most valuable. Telemanipulative systems such as that of the Da Vinci©are exceptions; however, these systems offer no capability of pre-operative planning transfer.

In an attempt to improve on the above concerns, the solution shown in Fig 1 was developed.

Fig. 1. Wheeled Robot Testing on Swine Skull

II. Methods

A. System Construct

The system construction was outlined in [6] as an optically tracked hand-held robot, with two spiked wheels on a single axis located either side of a craniotomy drill. The drill moves up and down tracking the bottom of the skull. This $\mathcal{Z}$ axis tracking is mechanically actuated through two springs maintaining upwards pressure on the drill. The drill is prevented from rising too far, by a Duraguard. The Duraguard is a piece of metal sitting under the drill axis; it both protects the brain from excessive penetration, and by extending slightly forward of the drill axis, provides a surface to track the bottom of the skull. See Figure 2. The two wheels are driven by two 25W brushless motors from Maxon Motor. The motors include embedded position sensors that feedback to PID controllers. The PID controllers are used to maintain the desired wheel velocity until the next control loop update.

The main body of this article is the kinematics and control algorithm that is used to determine the desired wheel velocities, without exact knowledge of the surface over which the robot traverses.

Fig. 2. Virtual view of Craniotomy Drill piece showing the Drill, which cuts the skull, and the Duraguard that protects the brain from the drill. The Duraguard is inserted below the skull, and tracks along it's bottom.

1) Shared control: The shared control of the robot exists through the delineation between the velocity, stability around the wheel axis, and the steering. The velocity of the robot is controlled in a push-pull way, similar to that of the Segway©. The surgeon pushes the robot in the desired direction, the robot hence leans forward, tilting around the wheel axis. The optical tracking detects this tilt, and increases the speed of the robot. The same works for stopping and reverse. The surgeon pulls back on the robot, the robot leans backwards, tilting around the wheel axis. The optical tracking sees this, and either stops the robot or reverses the robot along the trajectory. This is not just an intuitive speed control, but a shared control system in similar ways to those employing torque sensors for movement control of a robot arm.

2) Approach Overview: In order to gain all the required parameters for the control theory, the following approach is used:

```
Get 6DOF robot positions from optical
  tracking
Calculate robot positions in trajectory
  space
Determine current trajectory segment
Determine lateral offset of cutting axis
  from current trajectory segment
Determine angular error between forward
  motion of robot and trajectory
Determine sign of angular error
Determine intended velocity from robot
  tilt and surgeons intent
Determine desired angular control signal
Determine wheel velocities
```

B. Current Approach to Mobile Robot Kinematics

Mobile Robots with unicycle kinematics (i.e. dual wheels, single axis) are typically defined in terms of

the robots position $\mathcal{P}$ by $[x, y]$ and orientation ϕ given with respect to a world coordinate system also in 2 dimensions. The orientation defines rotation about an axis normal to the flat surface, and tilt of the robot around the wheel axis is often ignored. (The stability of these robots is often supported by a third or fourth off-axis wheel, though exceptions naturally exist.)

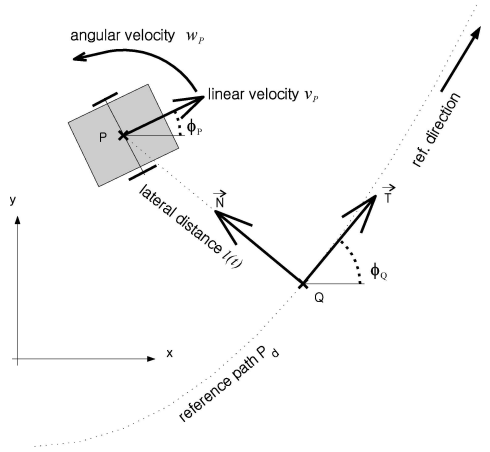

Fig. 3. Standard Mobile Robotics Parameters seen in the XY plane, from [7]

C. Approach Definition and Modification to 3D

For the robot in this paper, the use of 2D kinematics, is unfortunately too limited without modification. A skull's surface is 3D and predominantly non-linear. This means that the simple adoption to a spherical coordinate system is too limitied. Additionally in this project all parameters, including such aspects as robot tilt, need to be determined without knowledge of the target surface. Instead the following problem description is used.

The robot is modeled with the two wheels on a single axis moving on an arbitrary surface. In this architecture, the two identical wheels of radius r are mounted colinearly at a distance b and the robots position $\mathcal{P}$ is defined as the center of wheel axis. $\mathcal{P}$ needs to be defined by both position and orientation.

The aim of this project is however not the tracking of point $\mathcal{P}$ but instead the drilling axis which performs the craniotomy cut. The high speed drill performing this cut, is positioned several millimetres forward of $\mathcal{P}$ (at a distance c). The high speed drill can move along its own cutting axis, with the intent that it's tip tracks the bottom of the skull.

The cutting axis $\overrightarrow{\mathcal{C}_\mathcal{A}}$ is defined by two points, $\mathcal{C}_\mathcal{T}$ (Tip of the drill) and $\mathcal{C}_\mathcal{V}$ (Top of the drill). The forward direction of the robot is defined with a point $\mathcal{F}$ positioned forward of $\mathcal{C}_\mathcal{T}$. i.e with the vector $\overrightarrow{C_T F}$.

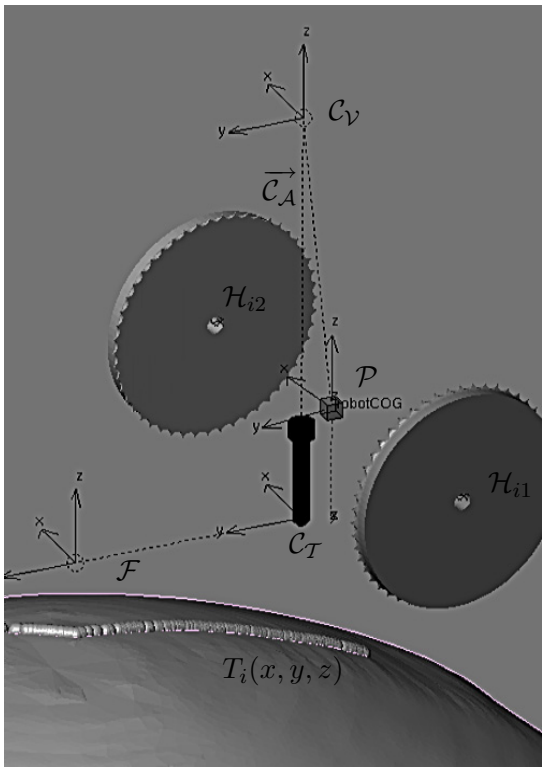

Fig. 4. Problem Definition for Craniotomy Cutting Robot, with exaggerated wheel offset b for clarity. The trajectory points $T_i(x, y, z)$ are shown as spherical markers on the surface of the skull.

The trajectory function for path following was defined as the series of points $T_i(x, y, z), i \in \{1..N\}$ where $N \in \mathbb{Z}$ is the number of points in the trajectory.

1) Lateral Offset: As with the 2D kinematics described above, it is necessary to determine the lateral offset $l(t)$ of the robot from the trajectory, and the angular error $\tilde{\phi}(t)$ between the robots heading and the desired trajectory. As the surface is unknown, the contact point of the drill with the skull is ignored. More directly the error distance $l(t)$ is determined by finding the minimum distance between the segments $\overrightarrow{\mathcal{C}_A}$ and $\overrightarrow{T_i T_{i+1}}$. (Here only the drill length segments may be used and not the complete vector projections. This is necessary to prevent false minimums occurring due to the cutting axis $\overrightarrow{\mathcal{C}_A}$ virtualling projecting from one side of the skull to the other side of the skull where another part of the trajectory may lie.) Similarly the trajectory segment $\overrightarrow{T_i T_{i+1}}$ must be used in order to prevent false minimums on concave shaped trajectories. The trajectory pair found at the minimum is labeled as $\overrightarrow{T_m T_{m+1}}$ The point on $\overrightarrow{\mathcal{C}_A}$ where this minimum occurs

is approximated to be where the intersection with the skull occurs, noted as $\mathcal{I}$.

2) Angular Error: The angular error $\tilde{\phi}(t)$, as with the 2D kinematics derivation, is defined as the angular error in the direction of motion. The angle between $\overrightarrow{T_m T_{m+1}}$ and $\overrightarrow{C_T F}$ includes components of tilt from the robot and cannot be used. As an example, it can be seen that the robot can drive forward almost completely leaned over. Here $\overrightarrow{C_T F}$ would point directly into the skull, and the angle between $\overrightarrow{T_m T_{m+1}}$ and $\overrightarrow{C_T F}$ would be $\approx 90\,^\circ$.

In order to remove the tilt component of the robot, two planes are defined. The first plane Π_1 for the robot is defined through points $\mathcal{F}$, $\mathcal{C_V}$ and $\mathcal{C_T}$. i.e. with a normal along the wheel axis, and independant of any tilt. The second plane Π_2 is defined by two vectors: the cutting axis, $\overrightarrow{\mathcal{C_T}\mathcal{C_V}}$ and the closest trajectory segment $\overrightarrow{T_m T_{m+1}}$. The angular difference between these two planes is used as the angular error $\tilde{\phi}(t) = cos^{-1}(\hat{n_1} \cdot \hat{n_2})$. This approach removes any error due to surface irregularities from height changes or roll of the robot from side to side (i.e. outside the plane Π_1).

3) Desired Velocity: In accordance with the initial intent for an intuitive control system, it was necessary to achieve a speed control by intepreting a native action of the surgeon.

The solution shown in Figure 5 was implemented using a weighted multiplication of three inputs. Two inputs come from an interface box we developed for the Aesculap High Speed Drill controller. From this box we determine firstly whether or not the surgeon wants the robot to do anything. i.e. A binary gated switch based on the foot pedal that controls the drill. Secondly we extract the torque of the drill motor. By knowing if the drill is having difficulty cutting, we decrease the forward speed, allowing longer time cutting. This decreases the forces on the wheels, and helps in maintaining traction.

As mentioned above for the shared control theory, the intent however comes mainly from a third input from the optical tracking. That being the tilt of the robot β around its wheel axis. We take β = 0 as the normal from the trajectory. This normal is defined from a third plane defined by two vectors, one taken as the cross product between the closest line between $\overrightarrow{T_m T_{m+1}}$ and $\overrightarrow{\mathcal{C_T}\mathcal{C_V}}$, and the second vector $\overrightarrow{T_m T_{m+1}}$. i.e. The normal to Π_3 is $\hat{n}_3 : (\overrightarrow{T_m T_{m+1}} \times \overrightarrow{\mathcal{C_T}\mathcal{C_V}}) \times \overrightarrow{T_m T_{m+1}}$

4) Angular Steering Control: Using $l(t)$, $\tilde{\phi}(t)$ and $v_P(t)$ from above an approach similar to that of [7] with details in [8] is used to determine the kinematic

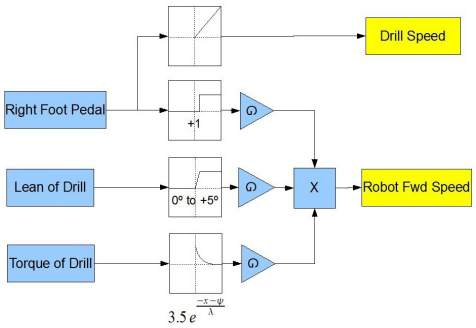

Fig. 5. Speed control determination for Robot

motion of the robot. A modified function for the desired angular velocity control signal $w(t)^*$ from [7] is shown in eq 1.

$$w^*(l(t), \tilde{\phi}(t), v_P(t)) = \frac{v_P(t) cos\tilde{\phi}(t)}{1 - l(t)} - \frac{k v_P(t) sin\tilde{\phi}(t)}{1 + (kl(t))^2} - (b_1) sat(\frac{z(t)}{\epsilon}) \quad (1)$$

$w(t)^*$ is the desired rotational velocity in rad/s around the drill axis. k , b_1 and ϵ are gain factors that determine the desired approach angle to the trajectory. $sat()$ is a saturation function between -1 and 1. z(t) is a sliding mode control function allowing the setting of a safety margin around the trajectory. The original function also included a $K(s(t))$ curvature function to accomodate for turns in the trajectory. This was removed because the trajectory here uses segments defined with sub-millimetre lengths, and the curvature between any two segments is very limited.

5) Wheel velocities: In order to convert this rotational velocity into wheel velocities, it needs to be shifted to the rotation around $\mathcal{P}$, the centre of the wheel axis. While the distance between the drill axis and $\mathcal{P}$ is a set distance, a direct shift cannot be employed. The problem is that due to the tilt of the robot, the drill axis can penetrate the skull forward or behind the centre of the wheels. This can lead to a complete reversal of the intended rotational velocity. Thus, an approximate position of the drill axis to skull penetration is determined, and a modified translation distance determined that takes the tilt into effect.

$$c_m = \frac{c - r sin(\beta)}{cos(\beta)} \quad (2)$$

The wheel velocities are then determined.

$$\begin{aligned} v_R &= sgn(c_m) w^* \sqrt{b^2 + c_m^2} + v_P \\ v_L &= -sgn(c_m) w^* \sqrt{b^2 + c_m^2} + v_P \end{aligned} \quad (3)$$

D. Optical Tracking

Within the desired application, the tracking of the robot and of the desired trajectory, are performed by optical markers residing on the top of the high speed drill, and on the head of the patient. The offsets of $\mathcal{C}_\mathcal{V}$ and $\mathcal{C}_\mathcal{T}$ are determined through a process of pivotisation. This involves the movement of a pointer about the desired point. The pointer has a seperately tracked marker set at it's end. The tracking of the marker set will extrapolate to a sphere. The centre of which is the point about which the item was moved. $\mathcal{F}$ is a virtual point that sits forward of the robot in the direction of movement. Here the robot is placed in a small jig that provides support against tilting (similar to providing training wheels forward and backwards), and driven forwards with equal wheel velocities. To remove any offset due to poor alignment of the training wheels, $\mathcal{F}$ is shifted in the z vector into the xy plane of $\mathcal{C}_\mathcal{T}$. The length of $\overrightarrow{\mathcal{F}\mathcal{C}_\mathcal{T}}$ is given unit length.

The position of the trajectory with respect to the marker body on the skull is determined through a rigid body registration, using the optical pointer pivotised on at least 3 titanium screws inserted into the skull, prior to surgery, and whose positions are known during the surgical planning.

In order to determine the robot position relative to the trajectory, it is necessary to translate the three positions $\mathcal{C}_\mathcal{V}$, $\mathcal{C}_\mathcal{T}$ and $\mathcal{F}$ by $\mathcal{H}_{RT}$. Using the translations from robot positions to robot marker as $\mathcal{H}_{\mathcal{C}_\mathcal{V}\mathcal{M}_\mathcal{R}}$, the robot marker to patient marker as $\mathcal{H}_{\mathcal{M}_\mathcal{R}\mathcal{M}_\mathcal{P}}$ and the translation from patient marker to trajectory as $\mathcal{H}_{\mathcal{M}_\mathcal{P}\mathcal{T}}$. These frames and translations are shown in Figure 6. In the trajectory coordinate system the robot positions are noted as (similar equations for $\mathcal{C}'_\mathcal{T}$ and $\mathcal{F}'$):

$$\mathcal{C}'_\mathcal{V} = \mathcal{C}_\mathcal{V} \times \mathcal{H}_{\mathcal{C}_\mathcal{V}\mathcal{M}_\mathcal{R}} \times \mathcal{H}_{\mathcal{M}_\mathcal{R}\mathcal{M}_\mathcal{P}} \times \mathcal{H}_{\mathcal{M}_\mathcal{P}\mathcal{T}} \quad (4)$$

III. Results

The testing of the Craniostar robot's control system for accuracy involved analysis of the robot's movement initially on flat surfaces, and then on phantoms skulls. The results of the tests are outlined in table 1. The measurements were made by laser scanning the surfaces after cutting. A comparison was made between the planned cut and the actual cut. The accuracy is defined as deviation of the cut width from the planned centre line, by more than the radius of the drill piece.

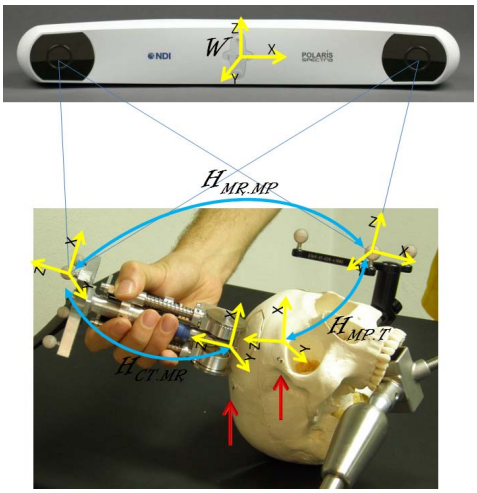

Fig. 6. Frame Determination and transformations shown for relevant bodies with IR reflecting optical tracking markers. (An earlier prototype of the robot is shown) The red arrows indicate the titanium skull markers used for pivotising the skull for registration.

A visualisation of this comparison is shown in Figure 7.

Two known inaccuracies lead to less than 100% of the accuracies under the 0.5mm region. The first in the initial placement of the robot. While the GUI can guide the surgeon in its placement, it is still found quite difficult to place the robot within 0.5mm of the start point. This initial placement is recovered quickly. For example see Fig 7) It is also noted that the initial burr hole used for insertion of the Craniotomy tool piece is larger.

The second error lies in the nature of the shared control of the system. The hand-held device is by nature prone to noise, specifically in external forces from the surgeons hand. Work is still being completed to identify the normal bounds of this noise and tune the control parameters more precisely. To date 20 tests have been performed on flat board and phantom skulls with an overall average of over 90% tracking $\leq$ 0.5mm.

IV. Conclusions and Future Works

1) Conclusions: In this paper, the control system applied to a new surgical robot system was described. The approach works effectively to provide 3D parameter determination for a robot moving without any regard for surface non-linearities.

The approach was tested on a variety of flat boards and phantom skulls. The tests have all proven positive in achieving accuracies that are equivalent to the larger modified industrial robot approaches, but with substan-

TABLE I

AVERAGE ACCURACIES ACHIEVED BY THE CRANIOSTAR ON DIFFERENT TRAJECTORIES

Surface	Trajectory	±0.5mm	±1mm
Flat Wood	Single straight 5cm segment	97.20%	100.00%
Flat Wood	Single curved 90 segment with 4cm radius	98.15%	100.00%
Flat Wood	Two 5cm segments joined with 45 join	97.60%	100.00%
Plastic Phantom Skull	Single straight 5cm segment	97.00%	100.00%
Plastic Phantom Skull	Single curved 90 segment with 4cm radius	95.00%	100.00%
Plastic Phantom Skull	Two 5cm segments joined with 45 join	95.60%	100.00%

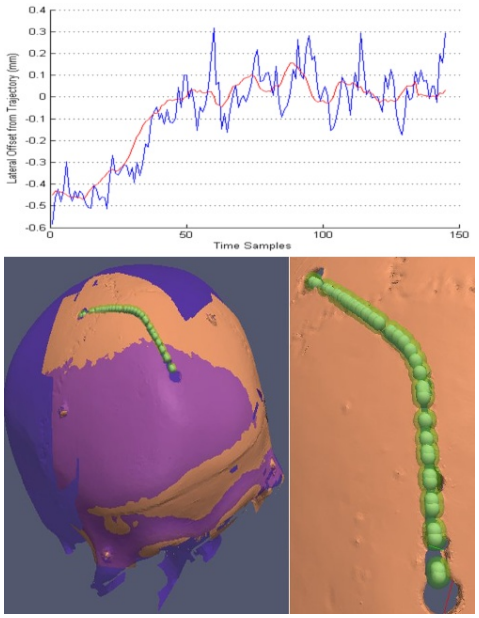

Fig. 7. Top picture is direct evaluation of tracking feedback for lateral error in the movement of robot with initial placement error, $l(t)$ (in blue) with a running average (in red). Under left picture is post cut evaluation through registration of pre-operation laser scan (blue) with post-operation laser scan (brown). This allows alignment of planned trajectory shown as green spheres. The transparent yellow surrounding spheres show the 0.5mm error boundary. The under right picture shows more detailed examples of the errors including the initial offset error, and approximately 1cm up from the burr hole, a handling error that resulted in a deflection to the right.

tially less impact on the OR, its real estate and the workflows of the surgeon.

2) Future Work: Work is continueing on assessing the accuracy of the robot in more complex trajectories (for examples see Figure 8), analysing more precisely the noise present due to the device being hand held, and methods for tuning the gain parameters of Eq 1 such that the bounded error can be maintained and the control guaranteed. A second area of research is in assessing the level of friction available on the skull. This is combined with methods for detecting slipage of the wheels.

A final prototype is now being built that further minaturises the system. This robot is designed to be completely sterilisable and ready for clinical trials.

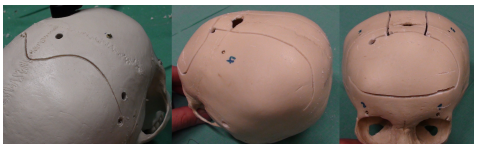

Fig. 8. Additional examples including at right a Fronto-orbital advancement with linear craniectomy.

REFERENCES

[1] Russel H. Taylor, Rajesh Kumar, and Patrick Jensen. Experiments with a steady hand robot in constrained compliant motion and path following. *Proceedings of the 1999 IEEE International Workshop on Robot and Human Interaction*, pages 92 – 97, 1999.

[2] S. Hassfeld and J. Muehling. Computer assisted oral and maxillofacial surgery, a review and an assessment of technology. *Int. J. Oral Maxillofac. Surg*, 30:2–13, 2001.

[3] S. Weihe, C. Schiller, C. Rasche, S. Hassfeld, M. Wehmaeller, H. Knoop, M. Epple, and H. Eufinger. Cad-cam prefabricated individual skull implants: new aspects in robot resection and guided bone regeneration. *International Congress Series*, 1268:584–590, 2004.

[4] D. Engel, J. Raczkowsky, and H. Wrn. Robacka: Ein robotersystem fuer den einsatz in der chirurgie. *Rechner- und sensorgestuetzte Chirurgie, Proceedings zum Workshop*, 4:279 – 286, 2001.

[5] P. Bast, A. Popovic, T. Wu, S. Heger, M. Engelhardt, W. Lauer, K. Radermacher, and K. Schmeider. Robot- and computer-assisted craniotomy: resection planning, implant modelling and robot safety. *Int J Med Robotics Comput Assist Surg*, 2:168–178, 2006.

[6] G. Kane, G. Eggers, R. Boesecke, J. Raczkowsky, H. Wrn, R. Marmulla, and J. Mhling. System design of a hand-held mobile robot for craniotomy. *MICCAI*, 2009.

[7] K. Seo and J.S. Lee. Kinematic path-following control of a mobile robot under bounded angular velocity error. *Advanced Robotics*, 20(1):1–23, 2005.

[8] C. Samson. Path following and time-varying feedback stabilization of a wheeled mobile robot. *Proc. Int. Conf. ICARCV92, Singapore*, RO13.1, 1992.